

Pre-processing Techniques to Improve the Efficiency of Video Identification for the Pygmy Bluetongue Lizard

Damian Tohl¹, Jim S. Jimmy Li¹ and C. Michael Bull²

¹*School of Computer Science, Engineering and Mathematics, Flinders University, South Road, Tonsley, SA, Australia*

²*School of Biological Sciences, Engineering and Mathematics, Flinders University, Bedford Park, SA, Australia*

Keywords: Video Identification, Pygmy Bluetongue Lizard, Curvature, DWT, SIFT.

Abstract: In the study of the endangered Pygmy Bluetongue Lizard, non-invasive photographic identification is preferred to the current invasive methods which can be unreliable and cruel. As the lizard is an endangered species, there are restrictions on its handling. The lizard is also in constant motion and it is therefore difficult to capture a good still image for identification purposes. Hence video capture is preferred as a number of images of the lizard at various positions and qualities can be collected in just a few seconds from which the best image can be selected for identification. With a large number of individual lizards in the database, matching a video sequence of images against each database image for identification will render the process very computationally inefficient. Moreover, a large portion of those images are non-identifiable due to motion and optical blur and different body curvature to the reference database image. In this paper, we propose a number of pre-processing techniques for pre-selecting the best image out of the video image sequence for identification. Using our proposed pre-selection techniques, it has been shown that the computational efficiency can be significantly improved.

1 INTRODUCTION

The Pygmy Bluetongue Lizard is an endangered species which was thought to be extinct for thirty years. They are found exclusively in remnant fragments of native grassland in South Australia's mid-north (Li et al, 2009), (Tohl et al, 2013), (Staugas et al, 2013), (Schofield et al, 2013). Identification of individual lizards is essential for ecological studies. One commonly used method is toe clipping. It is a highly invasive method whereby digits are removed from the feet of the lizards. The accuracy of this method can be affected by the fact that natural toe and foot loss can occur in lizards in nature (Hudson, 1996). Due to the Pygmy Bluetongue Lizards endangered status, a non-invasive identification method, such as photo identification using the Scale Invariant Feature Transform (SIFT) method (Lowe, 2004) is preferred.

As the Pygmy Bluetongue Lizard is an endangered species, there are restrictions on the amount of time a lizard can be captured for and the amount of handling. The lizards are captured in the field and placed in a Perspex box in which the video is captured and measurements are taken. There is

little control over the lighting conditions and their posture cannot be easily manipulated as the lizards are alive and constantly moving. It is therefore preferred to capture a video which is an image sequence of the lizard. However, it is very computationally inefficient to match every image in the sequence with every image in the database using SIFT, especially when the database could contain over hundreds of lizards. A number of pre-processing techniques are therefore proposed for pre-selecting the best image out of the image sequence of the video prior to identification of the lizard using SIFT.

From our experimental observation, the accuracy of SIFT identification depends on a number of factors including the degree of sharpness of the image and the difference of body curvature from the reference image in the database. Due to both camera and lizard movement and the time delay required to refocus by the camcorder, some images will be non-identifiable because of motion blur and out of focus. To determine the degree of sharpness of an image, the total energy of the high frequency components of the image is evaluated, based on the fact that sharp details contain high frequency components. The

discrete wavelet transform (DWT) was used to obtain detail coefficients in the horizontal, vertical and diagonal direction from which the total high frequency energy was measured.

Moreover, the true positive rate can be improved if the body curvature of the lizard is closer to that of the reference image in the database. For uniformity, all the reference images in the database are chosen to have a straight body. As a result, the image with the straightest body curvature out of the video sequence is to be chosen for identification. For curvature ranking, a series of morphological operations are used to obtain the skeleton of the lizard, and an index associated with the degree of curvature of the main body line is then determined. The best image for identification is selected by ranking the image sequence of the video according to an index, which is a combination of total high frequency energy and body curvature measurement, for each image. The best image selected from the video sequence in this way will produce the strongest match using SIFT.

The organization of this paper is as follows. Section 1 gives the introduction. In Section 2, the method for preparing the video sequence images prior to the pre-processing techniques is described. In Section 3, the pre-processing techniques including the high frequency energy and body curvature measurements are illustrated. The real and simulated experimental results are given in Section 4, and Section 5 gives the conclusion.

2 IMAGE PREPARATION PRIOR TO IDENTIFICATION

2.1 Lizard Image Segmentation

The first step in finding the best image from a video sequence is to convert the lizard video into a sequence of images. Interlaced video was captured by a full high definition camcorder with a resolution of 1920x1080 pixels. Since image identification does not require such a high resolution and in order to de-interlace the images, they are separated into odd and even fields. To maintain the original aspect ratio, the horizontal resolution of a field is scaled down by half by averaging every two pixels to produce one pixel so that the final resolution is 960x540 pixels. The averaging process is a part of the filtering for down-sampling the image and reducing any noise present and thus improving the accuracy of identification. The total high frequency energy of the de-interlaced image is then evaluated

for each field and the sharper one that has the higher total high frequency energy value is selected to be used in the video image sequence for identification. The averaging process will have an effect on the total high frequency energy, but will not affect the ranking of the images. It has been experimentally verified that this resolution is adequate for correct identification.

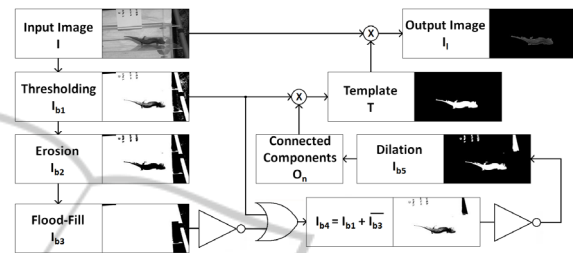


Figure 1: The flow chart of the method to produce a template to extract the lizard from the image background.

First of all, a binary template, T , that contains '1's where the lizard is located and '0's everywhere else is created to extract the lizard from the background in order to reduce identification errors. The method for producing the template and extracting the lizard is shown in Fig. 1. The original image, I , is converted to a binary image, I_{b1} , first by thresholding as given by (1).

$$I_{b1} = \begin{cases} 1, & I \geq L \\ 0, & I < L \end{cases} \quad (1)$$

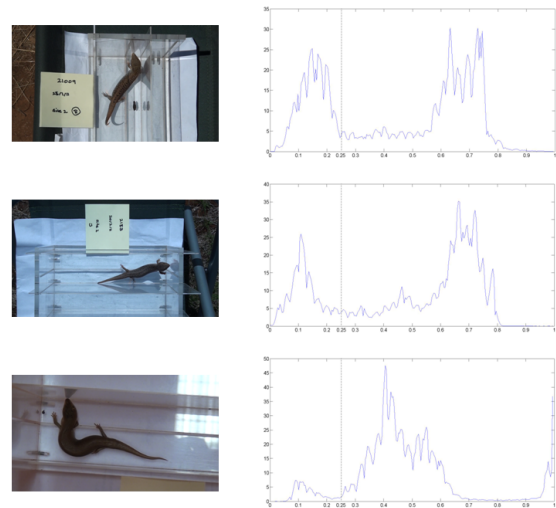


Figure 2: A single image from different sequences recorded under varying lighting conditions, and the corresponding histograms with the threshold value, $L = 0.25$.

It was found experimentally that $L = 0.25$ gave the best value for isolating the lizard due to the fact

the lizard is made up of mainly darker pixels. From Fig. 2, it can be seen in the image histograms that the threshold value $L = 0.25$ is appropriate to isolate the darker lizard object pixels under various lighting conditions.

In order to smooth the boundaries of the objects and also fill in any holes within the objects, a morphological erosion, Θ , is performed on I_{b1} in (2) to create I_{b2} .

$$I_{b2} = I_{b1} \Theta A^s \quad (2)$$

where $A^s = \begin{bmatrix} 1 & 1 & 1 \\ 1 & 1 & 1 \\ 1 & 1 & 1 \end{bmatrix}$ is the structuring element.

To remove unwanted features at the edges of the image, all other isolated objects located centrally, including the lizard, are first removed by applying a flood-fill morphological operation, F , (Soille, 1999) on I_{b2} in (3) to replace '0's by '1's to produce I_{b3} . The flood-fill morphological operation will replace '0's with '1's for those isolated background pixels within the image.

$$I_{b3} = F(I_{b2}) \quad (3)$$

The resulting image, I_{b3} , will now contain unwanted features at the edges without the lizard and can be used as a template to remove the unwanted features in which it contains by (4).

$$I_{b4} = I_{b1} + \overline{I_{b3}} \quad (4)$$

As a number of centrally located objects, including the lizard, are still remaining in the image, the lizard must be identified for extraction. $\overline{I_{b4}}$ is first dilated to smooth out edges and fill in any holes by (5) as follows.

$$I_{b5} = \overline{I_{b4}} \oplus A^s \quad (5)$$

where ' \oplus ' denotes morphological dilation.

Each image object, O_n , is then identified by searching for any 8-edge connected components in I_{b5} . Due to the scale pattern of the lizard, the object which relates to the lizard in the binary image has a region with a large fluctuation of black and white pixels, whereas other objects in the image are mostly homogenous regions with black pixels. Therefore the object in the binary image with the largest number of '1' pixels will be considered as the lizard. An array multiplication (i.e. element-by-element multiplication), denoted by, ' $*$ ', is performed between each object, O_n , and I_{b1} , and the number of '1' pixels is recorded as S_n , as given by (6).

$$S_n = \sum_{i,j} (O_n(i,j) * I_{b1}(i,j)) \quad (6)$$

The object that represents the lizard is considered to be O_n such that S_n is the maximum of $\{S_k\}$ where

$k = 1, 2, \dots, M$, and M is the total number of objects. This object can be used as the template image T given by (7).

$$T = \{O_n : S_n = \max\{S_k\} \quad k = 1, 2, \dots, M; 1 \leq n \leq M\} \quad (7)$$

The final lizard image, I_l , which has the background removed, is the result of an array multiplication of T and I , as given by (8).

$$I_l = I * T \quad (8)$$

3 BEST IMAGE SELECTION CRITERIA FOR IDENTIFICATION

3.1 High Frequency Energy Measurement

The discrete wavelet transform (DWT) is used to extract a value for the total high frequency energy of each image in the sequence. The one-dimensional scale function of the Haar family is defined as shown in (8), and the wavelet expression is given by (10).

$$\phi(t) = \begin{cases} 1, & 0 \leq t < 1 \\ 0, & \text{otherwise} \end{cases} \quad (9)$$

$$\psi(t) = \begin{cases} 1, & 0 \leq t < \frac{1}{2} \\ -1, & \frac{1}{2} \leq t < 1 \\ 0, & \text{otherwise} \end{cases} \quad (10)$$

The Haar wavelet is used to obtain the detail coefficients in the horizontal, vertical and diagonal directions, d^H , d^V , and d^D respectively. The sub-band image, a , is the approximation coefficients, but is only required for DWT calculation at the next scale. Fig. 3 shows the results of the wavelet transform, where the upper left quadrant corresponds to the approximation coefficients and the other quadrants correspond to the detail coefficients.

The amount of energy is calculated based on the Parseval Theorem, by the fact that the energy contained in the image is equal to the summation of the energy contained in the different resolution levels of the wavelet transform (Mallat, 1999).

As a result, the total high frequency energy corresponding to the detail coefficients is evaluated by (11) (Oliveira et al, 2010) as follows:

$$F = \sqrt{(d^H)^2 + (d^V)^2 + (d^D)^2} \quad (11)$$

To normalize the total high frequency energy, F , so that it does not depend on the size of the image

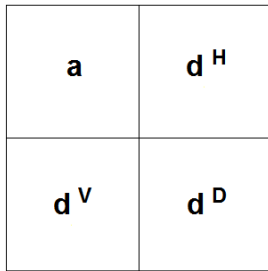


Figure 3: Two-dimensional wavelet coefficients.

for comparison, it is divided by the size, which is the total number of pixels, N , in the lizard, as given by (12).

$$G = \frac{F}{N} \tag{12}$$

where G is the normalized total high frequency energy.

An example of the total high frequency energy for a sharp image and a blurred image from the same image sequence is shown in Fig.4, it can also be seen that the number of SIFT keypoints is reduced in the blurred image.



Figure 4: A side by side comparison of a sharp and blurred image from the same sequence with the resulting total high frequency energy and SIFT keypoints.

Let G_k be the normalized total high frequency energy of the k^{th} image in the sequence. To further normalize the value of G_k between 0 and 1 so that it can be combined with its curvature index for ranking, each G_k value is divided by G_{max} , where $G_{max} = \max\{G_k\}$ where $k = 1, 2, \dots, p$ and p is the total number of images in the sequence.

The normalized total high frequency index of the k^{th} image, E_k , in the sequence is given by (13) as follows:

$$E_k = \frac{G_k}{G_{max}} \tag{13}$$

3.2 Curvature Index for Lizard Body

3.2.1 Limb Removal

An index associated with the degree of curvature of the lizard is also used to rank the best image. To determine the index, a line, representing the middle line of the body and limbs of the lizard must first be produced. This is achieved by applying a morphological dilation, \oplus , on the template and then follows by a morphological thinning operation, M , (Lam, Seong-Whan and Ching, 1992) in (14), to reduce its line thickness to a single pixel width producing the main body line, S .

$$S = M(T \oplus A^s) \tag{14}$$

As the curvature of the main body is only relevant, the lines that represent the limbs of the lizard in the main body line, S , have to be removed. In order to remove these limb lines, the intersection points are located and found. A square window centred at each intersection point is used to find the pixels that correspond to each line. For example, Fig 5(a) shows a square window centred at an intersection point. It has been experimentally found that a window size of 7×7 , is suitable for our application. If the window size is larger than 7×7 , too many unwanted pixels will be included, and the errors produced would lead to a higher false positive rate. If the window size is smaller than 7×7 , it is impossible to discriminate between the main body line and the limb.

To discriminate the main body line from the limb line, the pixels at the boundary of the square window together with the centre point, are used to construct three lines, as shown in Fig 5(b) and 5(c). If there are two connected pixels as shown in the top left corner of Fig 5(a), the pixel furthest from the centre is used. Each of the three lines has two angles associated with it, as shown in Fig. 5(c). Those angles can be determined using the cosine rule by (15). The line which has the smallest sum of angles is identified as the limb and is removed as shown in Fig. 5(d).

$$\theta = \cos^{-1} \left(\frac{a^2 + b^2 - c^2}{2ab} \right) \tag{15}$$

This process is repeated at each branchpoint until all the limb lines are removed to obtain the image, S_l . An example of the process used for limb removal is shown in Fig. 6.

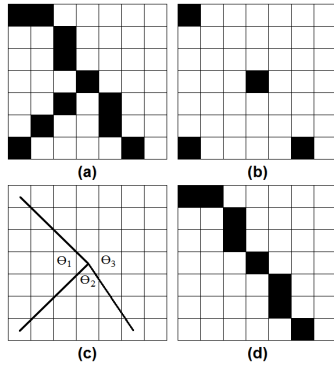


Figure 5: (a) The 7x7 window centred at an intersection point. (b) The pixels used to draw the lines. (c) The three lines and the corresponding angles. (d) The result after the line with the smallest sum of angles is removed.

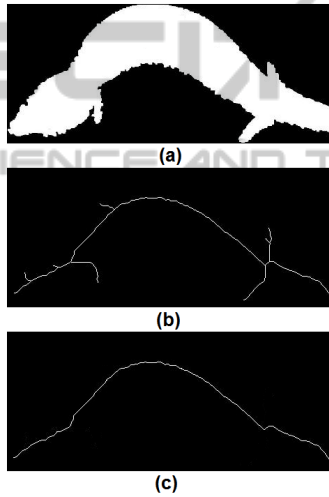


Figure 6: (a) The lizard template, T . (b) The main body line, S , after morphological thinning has been performed. (c) The resulting image, S_l , after limb removal.

3.2.2 Curvature Index

Variance is used to calculate the curvature index. The endpoints of, S_l , are found and the curve is rotated so that the line between the end points is horizontal.

The curvature index, C , is evaluated by the normalized variance of the curve given by (16), where y_j is the height of the curve at j , x_j is the position at j , x_p is the position at which y_j is maximum and N is the total number of elements in the curve. A lower variance value implies greater curvature of the lizard body. For a perfectly straight body, the normalized variance will give a value of unity.

$$C = \frac{\sum_{j=1}^N y_j (x_j - x_p)^2}{\frac{1}{N} \sum_{i=1}^N y_i \sum_{i=1}^N (x_i - x_p)^2} \quad (16)$$

3.3 Best Image Selection

To select the best image from the sequence, the normalized total high frequency energy index is combined with the curvature index for the k^{th} image using the harmonic mean equation given in (17) to generate a combined index value, Y_k .

$$Y_k = \frac{E_k C_k}{E_k + C_k} \quad (17)$$

where E_k and C_k are the normalized total high frequency energy and curvature indices of the k^{th} lizard image in the video sequence respectively.

The image with the largest combined index value Y_k in the image sequence is the best image chosen for identification.

By using the harmonic mean, both the normalized total high frequency energy index and the curvature index must be comparably large in order to give a large combined value of Y_k for a high ranking. If either one has a low value, the combined index will still be low and will remain low in the ranking.

4 RESULTS

4.1 High Frequency Energy Measurement

Experiments show that the number of SIFT keypoint matches is affected by the degree of blurring in an image. Both Gaussian and motion blur were tested by simulating the two different types of blurring on an image from the video sequence. The degree of blurring was simulated by gradually increasing the radius for Gaussian blur and by increasing the length for motion blur.

Table 1 shows the results of the blur simulation on a single image from a video sequence. In both cases, as the degree of blurring is increased, the number of SIFT matches decreases.

4.2 Curvature Index

It was found experimentally that for the strongest match, the body curvatures between the candidate and the reference lizard needs to be similar. Fig. 7 shows a database image on the left with different examples of body curvature in the images from a single sequence. The lizards with the straighter bodies that match the database image give a higher number of SIFT matches.

Table 1: Simulated Gaussian and motion blur with the corresponding number of SIFT matches and the normalized total high frequency energy, E_k .

Gaussian Blur				
Radius = 0	Radius = 1	Radius = 2	Radius = 3	Radius = 4
SIFT Matches 8	SIFT Matches 8	SIFT Matches 6	SIFT Matches 2	SIFT Matches 0
E_k 1.0000	E_k 0.5591	E_k 0.3478	E_k 0.2537	E_k 0.2009
Motion Blur (horizontal)				
Length = 0	Length = 1	Length = 2	Length = 3	Length = 4
SIFT Matches 8	SIFT Matches 7	SIFT Matches 4	SIFT Matches 2	SIFT Matches 0
E_k 1.0000	E_k 0.7927	E_k 0.6823	E_k 0.5802	E_k 0.5299

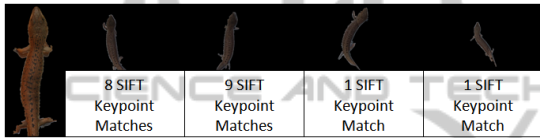


Figure 7: Examples of body curvature from a single image sequence versus the number of SIFT matches.

4.3 Best Image Selection

An example of an image sequence is shown in Fig. 8(a) and the images with the background removed and the main body line are shown in Fig. 8(b) and Fig. 8(c) respectively. The values for total high frequency energy and the curvature index for each image are shown in Fig. 8(d). From this example, it is obvious that Y_6 has the highest index value and would be used for identification.

In Fig. 8(c), it can be seen that the limb removal algorithm can produce a good approximation of the main body line for the evaluation of the curvature index for each lizard.

Table 2 gives the total time taken to process the complete video sequence of 150 images (approximately six seconds of video) using SIFT for finding a match versus the total time using our proposed method. It took approximately 1092 seconds to process the complete video sequence of images using SIFT while our proposed method took only 512 seconds on average to find a match from the video sequences. This is equivalent to cutting half the processing time. The experiments were performed on a windows 7 computer running an Intel Core i7 CPU @ 1.87Ghz with 8GB RAM.

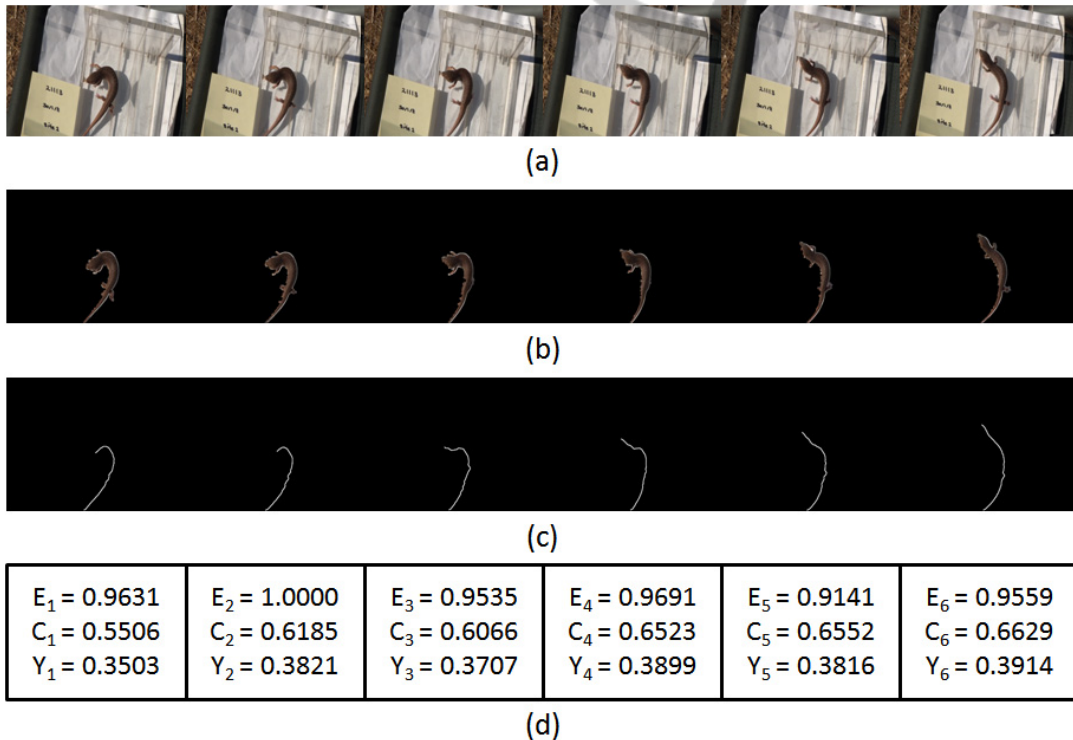


Figure 8: (a). An example of an image sequence. (b) The images after background removal. (c) The main body lines used for the curvature index. (d) The total high frequency energy, the curvature index and the resulting combined index values used for selecting the best image.

Table 2: Processing time for an image sequence of 150 images (seconds).

Sequence	1	2	3	4	5	6	7	8	9	10	Average
SIFT	1285	864	698	694	1171	1107	1191	1283	1310	1313	1092
Our Proposed Method	587	456	465	492	552	538	534	537	541	472	512

5 CONCLUSIONS

Pre-processing techniques to improve the efficiency of video identification for the Pygmy Bluetongue lizard using SIFT have been developed and found to reduce the time by half for finding a match. This will improve the efficiency for the identification process used for the continuing study of the endangered lizards and other species.

REFERENCES

- J. S. Jimmy Li, D. Tohl, S. Randhawa, L. Shamimi, C.M. Bull, 2009, "Non-invasive Lizard Identification using Signature Curves," 2009 *IEEE Region 10 Conference (TENCON 2009)*, pp. 1-5.
- D. Tohl, J. S. Jimmy Li, L. Shamimi, C. M. Bull, 2013, "Image Asymmetry Measurement for the Study of Endangered Pygmy Bluetongue Lizard".
- E. J. Staugas, A. Fenner, M. Ebrahimi, C. M. Bull, 2013, "Artificial burrows with basal chambers are preferred by pygmy bluetongue lizards, *Tiliqua adelaidensis*," *Amphibia-Reptilia*, vol. 34(1), pp. 114-118.
- J. Schofield, M. G. Gardner, A. Fenner, C. M. Bull, 2013, "Promiscuous mating in the endangered Australian lizard *Tiliqua adelaidensis*: a potential windfall for its conservation," *Conservation Genetics*.
- S. Hudson, 1996, "Natural toe loss in southeastern Australian skinks: implications for marking lizards by toeclipping," *Journal of Herpetology*, No. 30, pp. 106-110.
- David G. Lowe, 2004, Distinctive image features from scale-invariant keypoints. *Int. J. of Comp. Vis.*, 60(2):91-110.
- P. Soille, "Morphological Image Analysis: Principles and Applications," *Springer-Verlag*, pp. 173-174. 1999.
- S. Mallat, 1999, "A wavelet tour of signal processing," San Diego: *Academic Press*, p. 637.
- E. F. Oliveira, A. G. C. Bianchi, L. Martins-Filho, R. F. Machado, 2010, "Granulometric analysis based on the energy of Wavelet Transform coefficients," *Ouro Preto*, vol. 63(2), pp. 347-354.
- L. Lam, L. Seong-Whan, Y.S. Ching, 1992, "Thinning Methodologies-A Comprehensive Survey," *IEEE Transactions on Pattern Analysis and Machine Intelligence*, vol. 14, no. 9, pp. 879.